Journal of Power Sources 195 (2010) 6945–6953

Contents lists available at ScienceDirect

Journal of Power Sources

journal homepage: www.elsevier.com/locate/jpowsour

Potential improvement to a citric wastewater treatment plant using bio-hydrogen and a hybrid energy system

Xiaohua Zhi [a,b], Haijun Yang [a], Sascha Berthold [b], Christian Doetsch [b], Jianquan Shen [a,*]

[a] Beijing National Laboratory for Molecular Sciences, New Materials Laboratory, Institute of Chemistry, Chinese Academy of Science, Zhongguancun North First Street 2, Beijing 100190, PR China

[b] Business Unit of Energy Systems, Fraunhofer Institute for Environmental, Safety and Energy Technology UMSICHT, Osterfelder Strasse 3, Oberhausen 46047, Germany

ARTICLE INFO

Article history:
Received 11 February 2010
Received in revised form 14 April 2010
Accepted 14 April 2010
Available online 24 April 2010

Keywords:
Bio-hydrogen
Fuel cell
Hybrid energy system
Vanadium battery

ABSTRACT

Treatment of highly concentrated organic wastewater is characterized as cost-consuming. The conventional technology uses the anaerobic-anoxic-oxic process (A^2/O), which does not produce hydrogen. There is potential for energy saving using hydrogen utilization associated with wastewater treatment because hydrogen can be produced from organic wastewater using anaerobic fermentation. A 50 m^3 pilot bio-reactor for hydrogen production was constructed in Shandong Province, China in 2006 but to date the hydrogen produced has not been utilized. In this work, a technical-economic model based on hydrogen utilization is presented and analyzed to estimate the potential improvement to a citric wastewater plant. The model assesses the size, capital cost, annual cost, system efficiency and electricity cost under different configurations. In a stand-alone situation, the power production from hydrogen is not sufficient for the required load, thus a photovoltaic array (PV) is employed as the power supply. The simulated results show that the combination of solar and bio-hydrogen has a much higher cost compared with the A^2/O process. When the grid is connected, the system cost achieved is 0.238 US$ t^{-1} wastewater, which is lower than 0.257 US$ t^{-1} by the A^2/O process. The results reveal that a simulated improvement by using bio-hydrogen and a FC system is effective and feasible for the citric wastewater plant, even when compared to the current cost of the A^2/O process. In addition, lead acid and vanadium flow batteries were compared for energy storage service. The results show that a vanadium battery has lower cost and higher efficiency due to its long lifespan and energy efficiency. Additionally, the cost distribution of components shows that the PV dominates the cost in the stand-alone situation, while the bio-reactor is the main cost component in the parallel grid.

1. Introduction

Food processing industries usually discharge large volumes of wastewater characterized by high chemical oxygen demand (COD) or biological oxygen demand (BOD) [1]. Wastewater from the molasses process associated with the production of fodder yeast or citric acid is difficult to treat because of the presence of large amounts of organic matter [2]. Due to increased enforcement of discharge regulations and escalating surcharges by public owned treatment works (POTW), many food processing industries are taking steps to reduce, recycle or treat their wastewater before discharge [3]. Commonly the wastewater is treated by physical chemistry or biochemical methods, without renewable energy cycles. The emergence of biotechnology, which uses fermentative or/and photo-synthetic bacteria to consume the organic matter and produce biogas, such as hydrogen and methane, which can in turn be employed as an energy supply to the wastewater treatment process, may alleviate the burden of the wastewater industry [4,5]. In particular, hydrogen has acquired increasing attention as a "clean and green" energy carrier. A 50 m^3 pilot bio-reactor apparatus combining wastewater treatment and bio-hydrogen production was described by Yang et al. in 2006 [6].

The proton exchange membrane fuel cell (PEMFC) uses hydrogen and oxygen as fuels to produce energy alongside clean water production and is thought to be the ideal solution for pollution treatment and energy supply [7]. Currently, 90% of the world's hydrogen production is based on fossil fuels through steam reforming of natural gas, but the process releases large amounts of CO_2. Electrolysis is an alternative, but energy-intensive, way to produce hydrogen. By substitution of the power sources with renewable energy, such as photovoltaic or wind energy, the electrolysis process can be both eco-friendly and completely emission-free. Attention and interest in the design of hybrid energy systems that utilize photovoltaic and/or wind energy, as well as fuel cell (FC) sys-

* Corresponding author. Tel.: +86 10 62620903; fax: +86 10 62559373.
E-mail address: jqshen@iccas.ac.cn (J. Shen).

0378-7753/$ – see front matter © 2010 Elsevier B.V. All rights reserved.
doi:10.1016/j.jpowsour.2010.04.046

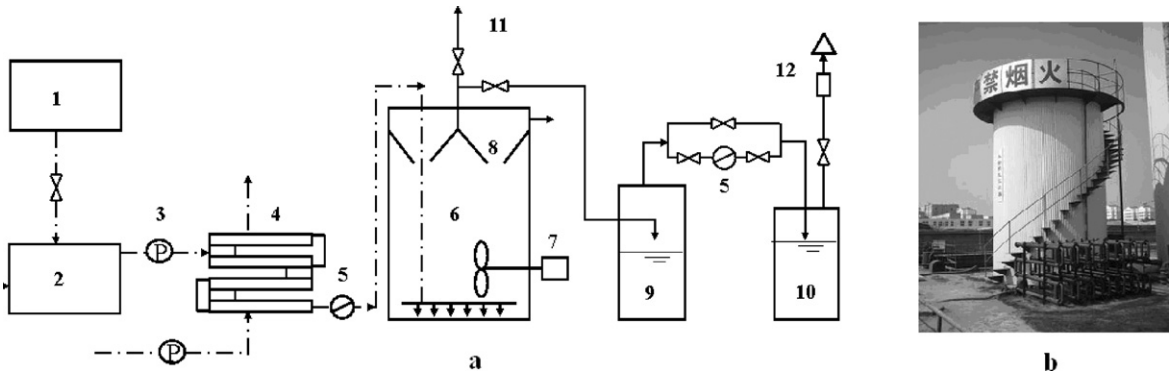

Fig. 1. Bio-reactor for hydrogen production: (a) schematic of bio-reactor. 1: NaOH storage; 2: suffer tank; 3: liquid pump; 4: heat exchanger; 5: liquid meter; 6; improved UASB reactor; 7: mixer; 8: gas/liquid/solid separator; 9: gas/water separator; 10: closed water excluder; 11: gas sampling port; 12: fire preventer [6]. (b) 50 m^3 bio-reactor in citric wastewater factory located in Shandong Province, China.

tems and/or battery storage systems have recently increased. Vosen and Keller [8] proposed the concept of a "hybrid energy storage system" and applied optimized control strategies for a stand-alone location. Compared with a single storage system, costs could be dramatically reduced by employing the solar powered, battery-hydrogen hybrid system (48% of the cost of hydrogen-only storage system and 9% of the cost of a battery-only option). On this basis, Li et al. [9] further developed the control strategy, size modeling and cost optimization. The proposed PV/FC/Battery hybrid system has been identified as the optimal configuration with lower cost, higher efficiency and less PV modules. Maclay et al. [10] have presented a dynamic model to evaluate a regenerative fuel cell (RFC) system with photovoltaic (PV) electricity generation. Cases of stand-alone and parallel grids were compared in meeting the dynamic demand of a family in California. Furthermore, these authors have used another storage component called an ultra-capacitor (UC) in the hybrid energy system [11]. The size, capital cost, control strategies and system efficiency were evaluated and it was found that preferential use of the RFC before the battery in meeting the load demand showed better performance compared with that before the RFC. In addition, an "Ecological House" with a hybrid energy system has been built in northern Italy, with control algorithms developed using fuzzy logic and an adaptive control strategy [12].

Although hydrogen can be produced cost-free from some organic wastewaters, few reports have been presented into using a combined bio-hydrogen and hybrid energy system, although similar work by Hedstroem et al. [13] in Stockholm has been reported with a solar-hydrogen-biogas-fuel cell system. The GlashusEtt includes a biogas burner and reformer, which can convert the nearby sewage water into hydrogen.

In our 50 m^3 pilot bio-hydrogen reactor (shown in Fig. 1) [6], the parameters of the reactor system and hydrogen yields have been listed in Table 1. This work is aimed at expanding upon current understanding and addresses the trade-offs associated with various combinations of energy systems, i.e. photovoltaic, bio-hydrogen, fuel cell and battery storage systems. Different system configurations (with/without a parallel grid) are analyzed and evaluated with respect to system efficiency and cost estimates. As a benchmark, the estimated cost of an anaerobic-anoxic-oxic process (A^2/O) is compared to evaluate the improved features. We aimed to simulate and estimate the combinations of energy devices in meeting the dynamic load demand.

Table 1
Database for the bio-hydrogen production system in citric acid wastewater factory [6].

Delivered by	Citric acid factory
Initial chemical oxygen demand (COD)	15,000–21,000 mg l^{-1}
Biochemical oxygen demand (BOD)/COD	0.56–0.68
Hydraulic retention time (HRT)	12 h
Volume of reactor	50 m^3
Volume loading rate (VLR)	38.4 kg COD m^{-3} d^{-1}
Hydrogen-producing rate per	0.72 m^3 H_2 m^{-3} d^{-1}
Hydrogen content in the biogas	36–38%
COD removal efficiency	72.4%
Total sugar degradation efficiency	96.6%

2. Components and modeling

2.1. Bio-hydrogen production system

High sugar degradation efficiency and COD removal efficiency were achieved and a massive 0.72 m^3 H_2 m^{-3} d^{-1} was generated in the citric acid wastewater plant, as shown in Table 1. The daily loading of wastewater is 106.67 t. The daily hydrogen yields were calculated as 36 m^3 based on the size of the 50 m^3 reactor.

It is also worth noting that only hydrogen and carbon dioxide were detected in the mixed biogas, without any methane, sulphide or carbon monoxide. The biogas enriched H_2 (36–38%) and CO_2 (62–64%) would be forced to flow through a combined alkaline absorption tower and, finally, hydrogen with purity of 99.995% can be accumulated for further utilization.

2.2. Compressor and hydrogen storage system

After purification in the combined alkaline absorption tower, hydrogen will be transported to the compressor and stored in the hydrogen tank. The rated power of the compressor depends on the pressure requirements for the inlet and outlet as well as the gas flow rate. The most efficient way to compress a gas is theoretically via an adiabatic process, as suggested by Hollmuller et al. [14].

In this study, the average gas flow rate was 0.42 L s^{-1}. The hydrogen density was 0.0899 kg m^{-3}. The inlet pressure of the compressor was set at 0.5 MPa based on the research of Shapiro et al. [15]. The outlet pressure was 5.0 MPa based on the charge pressure requirement of the hydrogen tank. The typical efficiency for the compressor was assumed to be 70% [8]. Thus, the rated power of the compressor can be estimated at 199.4 W. This means that 1 kWh of power consumption can compress 7.04 m^3 of gas under this condition.

The volume of the hydrogen tanks depends on the hydrogen yields, as well as the gas charge pressure and the gas discharge flow rate. In present work, the hydrogen yields per day were 36 m^3 under ambient pressure and temperature. When gas is charged to the tanks at 5.0 MPa, the required volume for the tanks was calculated

following the ideal gas law,

$$\frac{pV}{T} = nR = \text{constant} \quad (1)$$

where p is the absolute pressure, V is the volume of gas, n is the number of moles of gas, and T is thermodynamic temperature. The gas constant R is 8.314 J K^{-1} mol^{-1}.

Thus at 25 °C and 5.0 MPa, the required volume of the hydrogen tanks was calculated as 7.2 m^3. A 660-L hydrogen tank module from Rainer Lammertz was considered and 11 modules of hydrogen tanks were found to be sufficient to meet the storage demand [16].

2.3. Fuel cell system

The fundamental structure of a proton exchange membrane fuel cell (PEMFC) contains an anode (hydrogen as fuel supply) and a cathode (pure oxygen or air as fuel supply) separated by a solid membrane. The fuel cells were connected in series to meet the output voltage and power requirements. A DC/AC inverter was required for the power supply. The thermal energy is absorbed by a coolant loop directly connected to the accumulator tank. In our research, the optimal temperature for the hydrogen-producing microorganisms was in the range 30–35 °C. The wastewater from the citric factory should be pre-heated to meet the temperature adaption. Due to the thermal energy from fuel cell, the after-cooled water can be directly provided for the temperature control, which is very favourable for the energy saving.

As discussed above, abundant hydrogen is produced during the process of wastewater treatment. However, the size of a fuel cell should be rationally designed, considering the high initial investment of the fuel cell and the dynamic load demand. The modules of a fuel cell and detailed parameters can be found in Ballard [17]. The 4.4 kW fuel cell modules consist of 25 cells, which produce an output voltage of 15 V at 300 A. A typical efficiency for the fuel cell is 57%. The efficiency of the inverter in this work is 95%. In the round trip "hydrogen-compressor-hydrogen storage-fuel cell-load", the overall efficiency achieved is 37.9%. As we know, the low heat value of the hydrogen (LHV) is 33 kWh kg^{-1}. Based on the daily hydrogen yields of 36 m^3, the average power output is calculated as 40.22 kWh.

2.4. Photovoltaic array and electrolyzer

The photovoltaic module can be placed on the roof of a building, to convert the sun's rays or photons directly into electrical energy. The output power is easily increased when connecting the module in series. The Shandong province is located at the 37.32 N latitude and receives an average daily solar power density of 3.3–4.1 kWh m^{-2} or, annually, 1200–1500 kWh m^{-2}. The typical solar radiation occurs between 09:00 and 17:00 h [18]. The abundant solar energy resources could supplement the load when the electricity produced by the fuel cell cannot meet the demand. On the other hand, the size of the PV module should be optimized because of the high initial investment. Detailed parameters for the PV module can be obtained from Naps Systems Oy [19].

Furthermore, solar radiation is distributed differently during sunrise, midday and sunset. Therefore, when a system is operated without battery storage, the excess electricity generation should be supplied to the electrolyzer to avoid energy wastage. A typical efficiency of an electrolyzer has been suggested at 74% [9]. In the round trip "PV-electrolyzer-compressor-hydrogen storage-fuel cell-load", the total efficiency was calculated as 28.05%.

2.5. Battery storage system

Battery storage technology is recognized to have significant potential in utility scale applications, especially for load leveling and peak shaving. The batteries are rated in terms of their energy and power capacities, as well as other important features, efficiency, life span (stated in terms of number of cycles), operating temperature, depth of discharge, self-discharge and energy density.

Lead acid battery has developed in a long history and has been used widespread due to their low cost. However apparent disadvantages such as short life cycle and low discharge depth also limit their applications for the higher load demand and the long-term energy storage. Vanadium redox flow battery is a type of electrochemical storage device which owns separate energy and power rating. The energy rating depends on the size of the electrolyte tanks, while the power rating depends on the size of cell stack and numbers of the cell module. Fraunhofer society develops the vanadium redox flow battery. The single cell owns 2025 cm^2 electrode area. The voltage has been charged to maximum 1.68 V at 50 mA cm^{-2} in order to avoid the damage to the electrode and membrane. After that, the cell has been discharged to a voltage of 0.9 V at 50 mA cm^{-2}.

In China, the peak time price was 0.154 US$ kWh^{-1} between 08:00 and 22:00 hrs and the valley price was 0.069 US$ kWh^{-1} the other times. The wide difference between peak and valley electricity prices apparently favours the use of batteries as supplemental power sources, which act as load leveling and/or peak shaving devices. In this work, both lead acid and vanadium batteries were considered and compared for meeting the load demand related with the cost analysis and lifespan.

2.6. Cost estimates

Efficiency, capacity, cost, lifespan and O&M costs of components are summarized in Table 2. The estimates are based on previous reports, industry inquiry and temporary market tendencies. After sizing the components to meet the required load, the initial investment and electricity cost are calculated from Eqs. (2)–(5). It is noted that the calculated cost represents a rough estimate for the system. However, to some extent, it describes the possibilities under variable operation.

The total initial investment is calculated as

$$C_{i,c} = \sum_{\text{components}} (C_{\text{cap, comp}} \times S_{\text{comp}}) \quad (2)$$

where $C_{i,c}$ is the total initial investment, $C_{\text{cap,comp}}$ is the capital cost of components and S_{comp} is the size of components.

For an individual component, the annualized cost is calculated using Eqs. (3) and (4), and the average electrical cost is given by Eq. (5):

$$f_{\text{annu}} = \frac{i}{(1+i)^n - 1} + i \quad (3)$$

$$C_{\text{acomp}} = C_{\text{i,c, comp}} \times f_{\text{annu}} + C_{\text{aom, comp}} \quad (4)$$

$$C_{\text{coe}} = \sum_{\text{components}} \frac{\text{cost} \times \text{size}}{\text{lifespan} \times \text{annual electricity usage}} \quad (5)$$

where i is the real interest rate (5% in this work), f_{annu} is the annualized factor, n is the lifespan of the component, C_{acomp} is the annualized cost of the component, $C_{\text{i,c,comp}}$ is the initial annualized cost of the component and $C_{\text{aom, comp}}$ is the annual O&M cost of the component. Finally, C_{coe} is the average cost per kWh of electricity.

The technical parameter is defined as system efficiency by dividing the output energy by the input energy.

Table 2
Component efficiencies, cost, lifespan, and O&M cost [9,20,21].

Component	Efficiency (%)	Cost (US$)	Lifespan (year)	O&M cost (% of the investment cost)
Bio-reactor	100	24,286	20	16.5
CO_2 absorption tower	95	2286	20	31.5
Compressor	70	2500 kW^{-1}	10	2.0
Hydrogen Tanks	100	30 kWh^{-1}	20	0.5
Fuel cell	57	2500 kW^{-1}	≤40,000 h	2.5
Inverter	95	720 kW^{-1}	10	0.5
PV	13.5	4300 kW^{-1}	20	0
Electrolyzer	74	1000 kW^{-1}	10	2.0
Lead acid battery	72 (DOD = 70%)	110 kWh^{-1}	3	3.0
Vanadium battery	80 (DOD = 75%)	500 kWh^{-1}	15	1.0

In the stand-alone situation, system efficiency is calculated as

$$\eta_{\text{system}} = \frac{E_{\text{load}}}{E_{\text{PV}} + E_{\text{H}_2,\ \text{produced}} + E_{\text{battery,\ consumed}}} \quad (6)$$

When systems are connected with grid, system efficiency is calculated as

$$\eta_{\text{system}} = \frac{E_{\text{load}} + E_{\text{to grid}}}{E_{\text{H}_2,\ \text{produced}} + E_{\text{battery,\ consumed}} + E_{\text{from grid}}} \quad (7)$$

where the load, PV, H_2 produced from bio-reactor, energy consumed by battery, and the energy from/to grid are all defined in kilowatt-hours (kWh).

3. Results and discussion

The schematic of the hybrid energy system in this work is presented in Fig. 2, including components, inverter, central control system and seven controlling subsystems. Variable operations could be designed based on the different control strategies.

3.1. Load demand of the bio-reactor system and rated 50 kW solar array output

The load demand of the wastewater treatment system was recorded on 15 October 2006 in Shandong Province. The power output from the rated 50 kW solar arrays was measured in Jiangan PV station [22]. The results are used and analyzed in this work when considering their locations at similar latitude and similar solar resources. The load demand and PV output are presented in Fig. 3. The total electricity required for the reactor system was 53.14 kWh and the total energy supplied by the PV array was 28.6 kWh. It is apparent that peak demand appears regularly every 4 h, because the wastewater is pumped into the reactor every 4 h. Approximately an average 2.5 kW power supply is required to meet the daily power demand. Additionally, the maximum peak demand is as high as 4.22 kW and the power supply must be sufficient to sustain successful operation at peak hours. As discussed previously, the fuel cell alone cannot meet the total load as the daily generation is 40.22 kWh. Either grid connection or other energy resources must be supplied as required for the system to function.

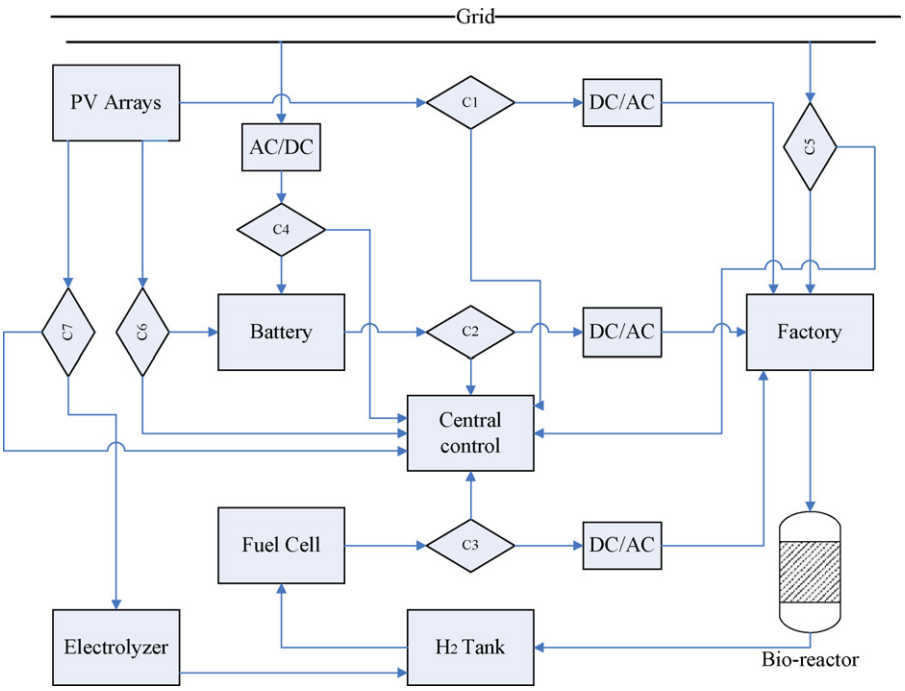

Fig. 2. Schematic of the hybrid power systems: C1, controlling subsystem for solar energy; C2, controlling subsystem for battery; C3, controlling subsystem for fuel cell; C4, controlling subsystem for grid to charge the battery; C5, controlling subsystem for grid connection; C6, controlling subsystem for PV to charge the battery; C7, controlling subsystem for PV to electrolyzer.

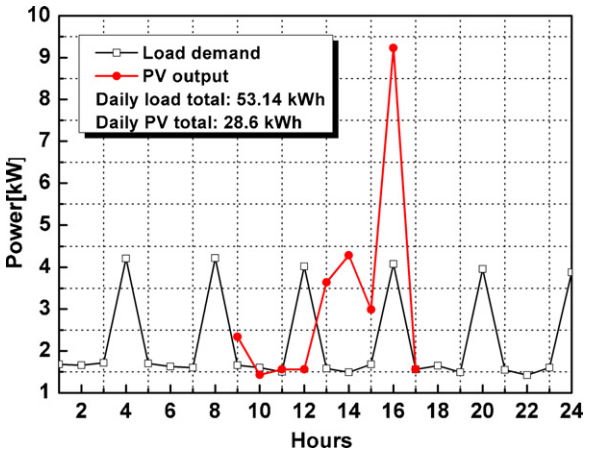

Fig. 3. Load demand of system on 15 October 2006 and rated 50 kW PV power output.

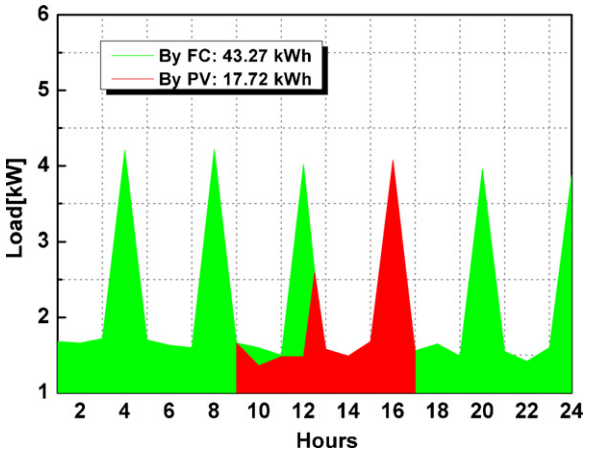

Fig. 4. Fraction of total load demand met by PV and fuel cell in the stand-alone situation when using rated 50 kW PV and rated 4.4 kW fuel cell.

3.2. Stand-alone analysis

In the stand-alone situation, there is no power exchange with the grid. Thus an extra energy supply is needed to cover the deficit between load and fuel cell. A PV array is preferable for filling the gap. However, it should be noted that there is no solar power available in the morning or evening, while excess solar energy is available at midday. Two configurations can be considered to consume the excess solar energy at peak radiation. First, the excess PV output can be provided to an electrolyzer. This system is called the PV/FC system. The other process employs a battery to store the excess PV energy at peak hours, which is called the PV/FC/Battery system.

3.2.1. PV/FC system

The daily hydrogen yield is thought to be constant because of the steady operation of the bio-reactor. The PV station also provides the electricity to the load when the fuel cell is out of supply. The typical solar radiation in October occurs between 09:00 and 17:00 h. From our results, it is clear that between 09:00 and 12:00 h the PV power cannot sufficiently meet the load demand and in contrast between 13:00 and 17:00 h, the large excess PV output should be stored. In the PV/FC system, the electrolyzer is used to consume the excess solar output for hydrogen production and fuel cell runs during the rest time to meet the load demand. The system configuration shown in Fig. 2 includes the C1, C3 and C7 controlling subsystems. The simulation of each power fraction for the total load demand is presented in Fig. 4. As peak demand is at 4.22 kW, the minimum output from the fuel cell should be 4.22 kW when it is operated without available solar radiation. In this simulation, the power-rated 4.4 kW modules from the Ballard Fuel Cell were employed. The output voltage was 15 V DC. The power was connected with load through the inverter (24 V DC to 220 V AC, 50 Hz). Between 09:00 and 13:00 h, the energy gap between the PV and the load was 2.88 kWh, which can be compensated by the fuel cell. The excess solar energy during this time was 10.88 kWh. When the electrolyzer was used, the calculated electricity generation was 3.05 kWh, based on a round trip efficiency of 28.05%, which means that the deficit at low solar radiation could be sufficiently covered by electrolysis. The total electricity produced from the PV/FC system was 60.99 kWh.

As we know, the energy from a fuel cell can be divided into two parts: electricity generation and thermal output. When considering the accompanying heat generation, it would definitely save energy to exchange heat from the after-cooling water with the wastewater substrate, as the optimized cultivated temperature for the microorganisms is 30–35 °C. However, the PEMFC stacks lose some part of its generated heat to the environment by means of convection and radiation. The typical loss efficiency takes about 19% of the total generated heat according to a report from Xie et al. [23]. The calculated thermal energy of cooling water per day is 190,926 kJ. In this scenario, when the ambient temperature is 298.15 K and it is heated to 303.15 K, the fuel cell stack can satisfy approximately 7806.4 kg cooling water for the temperature adjustment of wastewater.

3.2.2. PV/FC/battery system

In this configuration, the PV array also serves as the extra energy supplier. However, a battery, not the electrolyzer, was used to store the excess solar energy at high radiation and release it when the load demands. The control strategy is composed of C1, C2, C3 and C6 subsystems. The design is based on the consideration that the process of the PV-electrolyzer-hydrogen-fuel cell possesses a low system efficiency of 28.05%. In contrast, the process of battery storage produces higher round trip efficiency, of 76% for the vanadium battery and 68.4% for the lead acid battery. On the other hand, the regular peak load requires high rated power from the fuel cell, as well as a high initial investment. As the battery has the excellent capabilities of peak shaving and load leveling, it is natural to use a battery to cover the peak demand and sustain a steady fuel cell output at the lower rated power. This is important to prolong the lifespan of the fuel cell. It should be noted that batteries cannot exceed their limit of state of charge (SoC) as well as limitations on battery depth of discharge (DoD), to maintain better battery

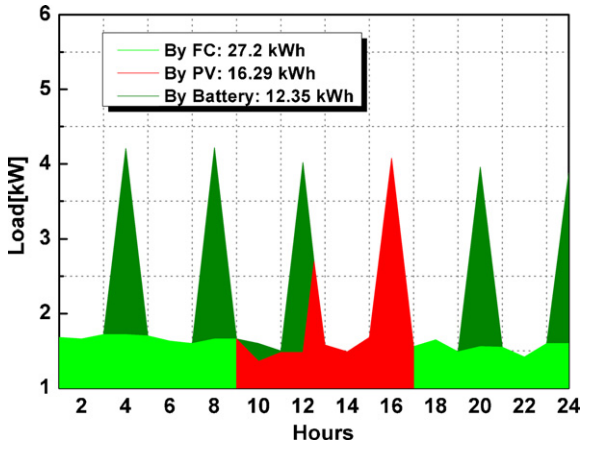

Fig. 5. Fraction of total load demand met by PV, fuel cell and battery in the stand-alone situation when using rated 50 kW PV, rated 1.7 kW fuel cell and 15.6 kWh battery (vanadium battery) or 18.6 kWh battery (lead acid battery).

Table 3
Parameters and cost analysis for PV/FC system and PV/FC/Battery system in stand-alone analysis.

Stand-alone Analysis	PV/FC system	PV/FC/Battery system	
		Lead acid battery	Vanadium battery
Initial Investment (US$)	256930.4	251266.4	257020.4
Total annual cost (US$)	26937.5	26106.2	26122.8
Electricity cost (US$ kWh^{-1})	1.299	1.261	1.245
System cost (US$ t^{-1})	0.692	0.671	0.671
System efficiency (%)	39.5	39.9	40.7

performance with respect to power density and efficiency. In this scenario, the fuel cell is operated at a rated power of 1.7 kW and the deficit at peak load is supplied by the battery. The simulation system is presented in Fig. 5. From 13:00 to 17:00 h, 10.88 kWh electricity was stored in the battery. When discharged, 8.38 kWh can be supplied for the load, which is much higher than the process of electrolysis. The total electricity achieved in this system was 64.86 kWh. The power supply is sufficient to meet the load demand under this operation.

The initial investment, annual cost, electricity cost, system cost and system efficiency for the stand-alone analysis are summarized in Table 3. A cost estimate for the A^2/O process is shown in Table 4. It is apparent that the stand-alone system with PV requires a high initial investment, annual cost and system cost, compared with the A^2/O process. When a battery is used, it enables peak shaving, which reduces the required size of the fuel cell. In particular, when we consider the long durability of the vanadium battery, it has an advantage in comparison to the process of electrolysis. The results are in accordance with the previous result reported by Vosen and Keller that the electricity cost could be reduced when a hybrid energy system is employed compared to a single storage system [8].

In addition, two types of batteries were estimated and compared when they functioned as peak shaving storage devices. Based on the parameters in Table 3, it is apparent that the cheaper lead acid battery naturally possesses a comparatively low initial investment. However, if we consider the lifespan of the battery, the vanadium battery gradually reveals an excellent property due to its long lifespan and high discharge depth. At present work, 72% DoD is assumed for the lead acid battery. In practice, the DoD of a lead acid battery is normally controlled at a low level to prolong the battery lifespan, which means that the designed capacity for lead acid battery should be enlarged to store the required energy. Thus, the initial investment for the lead acid battery should be higher than our design in this work. In contrast, the high discharge depth of the vanadium battery entirely satisfies a constant performance and cost reduction over the long-run.

3.3. Parallel grid analysis

3.3.1. FC system

In the scenario of a parallel grid, the load is met by a grid connection when the power output from the fuel cell is not sufficient. In China, the electricity price varies between peak hours and valley hours, at 0.154 and 0.069 US$ kWh^{-1}, respectively. The initial idea was to employ the fuel cell at peak hours and for the grid to serve the load during valley hours. The control strategy is under the operation of the C3 and C5 subsystems as shown in Fig. 2. The simulated operation can be found in Fig. 6. From 08:00 to 22:00 h, the total load demand was 33.46 kWh and the output from the fuel cell was 40.22 kWh. This means that the fuel cell can sufficiently cover the load demand at peak hours. As the reactor will stop running with power outages, the power output from the fuel cell should be sized up to 4.2 kW at least. During valley hours, the electricity supplied by the grid is calculated as 23.81 kWh to meet the load, considering the electricity consumption of the compressor at 5.11 kWh and the inverter at 4.8 kWh.

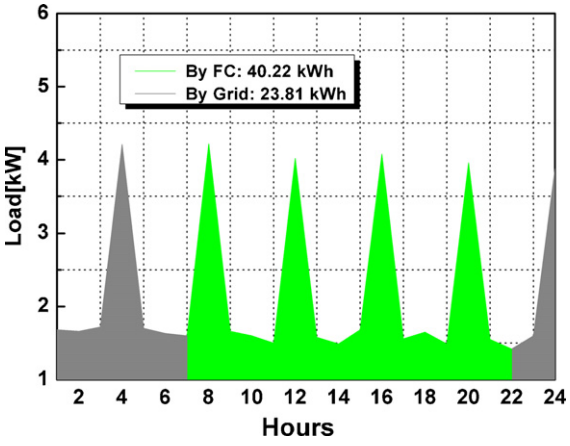

Fig. 6. Fraction of total load demand met by fuel cell in grid parallel when using rated 4.4 kW fuel cell.

Batteries and fuel cells possess natural advantages of load leveling and peak shaving, allowing deferral of generation expansion and investment increase. In the reactor system, the peak demand appeared regularly every 4 h. To reduce the investment in the fuel cell, the control should level the output from the fuel cell at the lower rated power and the grid serves as the supplement for the deficit between the load and the fuel cell. The simulation is presented in Fig. 7. When the 1.7 kW rated fuel cell is utilized for the supply, there is a substantial decrease in initial investment. Furthermore, a constant and regulated operation is easy to control, which is, to some extent, beneficial to prolong the durability of the fuel cell. In this scenario, the electricity required from the grid was 26.29 kWh.

The initial investment, annual cost, electricity cost, system cost and system efficiency are summarized in Table 5. As assumed, the system with a lower rated power of fuel cell shows a lower initial investment and annual cost. This is attributed to the leveling of the

Table 4
Cost analysis for the A^2/O process.

Type	Total annual cost (US$)	System cost (US$ t^{-1})
A^2/O process	10006.2	0.257

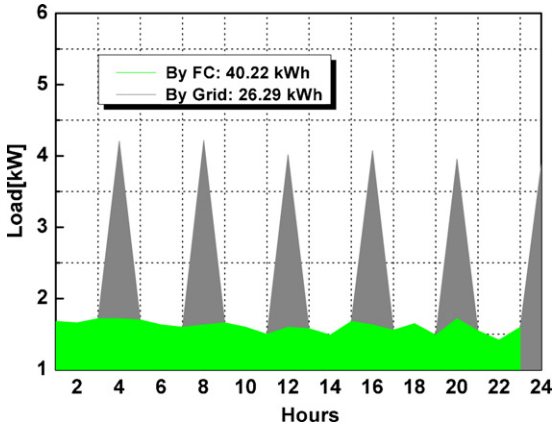

Fig. 7. Fraction of total load demand met by fuel cell in grid parallel when using rated 1.7 kW fuel cell.

Table 5
Parameters and cost analysis for FC (rated 4.4 kW)/grid system, FC (rated 1.7 kW)/grid system and FC (rated 1.7 kW)/grid/battery system, as well as the costs of solar-hydrogen in the world.

Grid parallel analysis	Initial investment (US$)	Total annual cost (US$)	Electricity cost (US$ kWh^{-1})	System cost (US$ t^{-1})	System efficiency (%)
FC (rated: 4.4 kW)/grid	40970.4	10194.1	0.245	0.262	48.5
FC (rated: 1.7 kW)/grid	34270.4	9258.7	0.197	0.238	47.6
FC/grid/lead acid battery	36376.4	9648.4	0.279	0.248	47.1
FC/grid/vanadium battery	42470.4	9591.0	0.261	0.246	48.2
Southern European[a]			0.43		
Northern European[a]			0.86		
China[a]			1.00		

[a] The data are based on the work by Liu et al. [24].

fuel cell based on the specific load character. The cost of wastewater treatment with a 4.4 kW fuel cell was 0.262 US$ t^{-1}, which is slightly higher than the cost of the A^{2}O process at 0.257 US$ t^{-1}. However it is worth mentioning that the system cost has been reduced significantly compared with the PV surplus system in the stand-alone situation. When the fuel cell was rated at 1.7 kW, the system cost was 0.238 US$ t^{-1}, which is lower than the cost of the A^{2}O process, including the annual cost. The operation is ideal not only for cost considerations but also beneficial for energy saving and sustainable development. In addition, it is apparent that the electricity cost of bio-hydrogen is much lower than the reported cost of solar-hydrogen as presented in Table 5. The results reveal that hydrogen from biomass can be more economical than hydrogen from solar energy.

3.3.2. Hybrid battery/FC system

As suggested by Vosen and Keller, the electricity cost could be reduced when a hybrid energy storage system is utilized compared with a sole storage system [8], we used a battery system to shave the peak demand and level the fuel cell output at peak hours in consideration of the higher electricity price. The system configuration is presented with C2, C3, C4 and C5 subsystems. The grid provides the electricity output at valley hours, and meanwhile charges the battery. Power output from the fuel cell is regulated at 1.7 kW, to meet the load and consumption of the compressor. At peak hours, the battery is discharged to meet the peak demand. Under this operation, the required power from the fuel cell is 27.2 kWh, from the grid is 24.64 kWh and from the battery is 10.19 kWh, as shown in Fig. 8.

The lead acid battery and vanadium battery were also used to compare the long-term operation and cost estimates. As presented in Table 5, the vanadium battery shows a higher initial investment, whereas it possesses a lower annual cost and electricity cost. It is apparent that the vanadium battery has higher efficiency and life span. The system cost for the vanadium battery system was 0.246 US$ t^{-1}, which is still higher than the FC (rated 1.7 kW)/grid system at 0.238 US$ t^{-1}. This is attributed to the high investment of the battery system. In the vanadium battery system, the electrolyte comprises about 35.0% of the total cost, suggesting that the system cost is substantially sensitive to the market price of vanadium pentoxide. The price was predicted to decrease with larger exploitation of mines and industrial scale production of the electrolyte. On the other hand, the lead acid battery cannot be operated long-term and at deep discharge because of the need to sustain their limited durability. Thus the battery capacity should be larger, designed to meet the low discharge level, which also requires an increased investment. In the long-run, it can be summarized that a vanadium battery demonstrates its synthesized advantages for energy storage.

Optimized operations for 1 week starting the 15 October 2006, under stand-alone and parallel grid situations were simulated and are shown in Figs. 9 and 10, respectively. The operations are satisfactory and cost-effective in meeting the dynamic load demand based on the above analysis. In the stand-alone situation, the PV array, fuel cell and battery are employed to regulate the dynamic behavior. When the system is connected to the grid, the fuel cell serves to level the load during peak hours.

3.4. Sensitivity analysis of component costs

The costs of wastewater treatment under different operating conditions are presented in Fig. 11 and the cost distribution of components in Fig. 12. When the plant is grid independent, the system cost and electricity cost are much higher than that in a parallel grid. It is apparent that the expensive investment of the PV array causes an increased system cost, of about 60% above the system cost

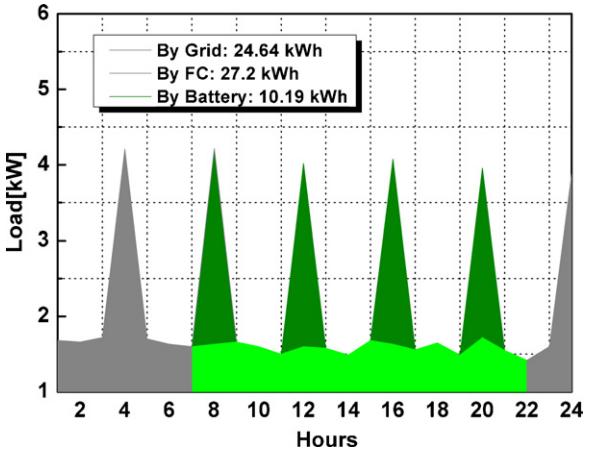

Fig. 8. Fraction of total load demand met by fuel cell and battery system in grid parallel when using rated 1.7 kW fuel cell and 16.5 kWh battery (vanadium battery) or 19.6 kWh battery (lead acid battery).

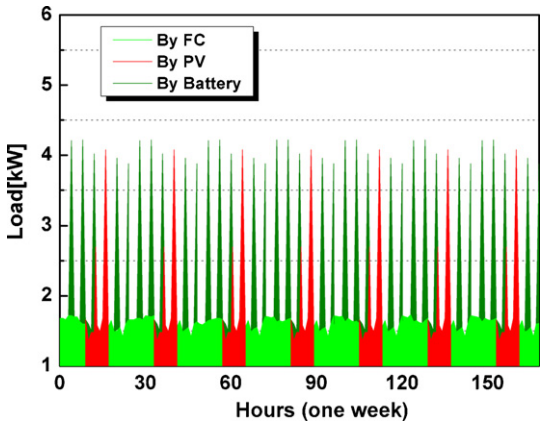

Fig. 9. Load demand met by rated 50 kW PV array, rated 1.7 kW fuel cell and 15.6 kWh vanadium battery plotted over 1 week in the stand-alone situation.

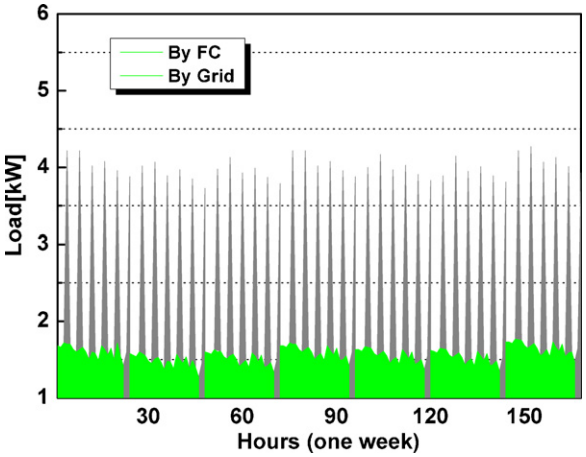

Fig. 10. Load demand met by rated 1.7 kW fuel cell, 16.5 kWh vanadium battery and grid connection plotted over 1 week in the grid parallel.

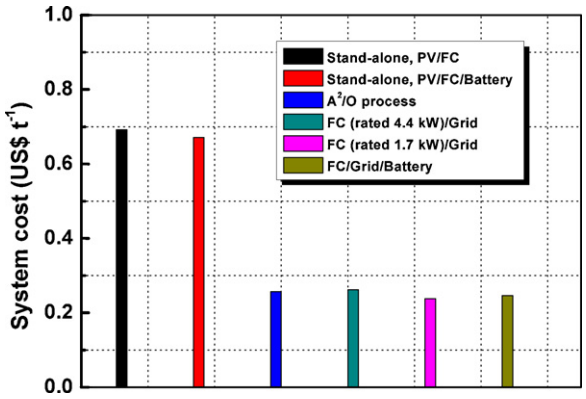

Fig. 11. Cost of wastewater treatment under different operations. The estimated cost is based on the vanadium battery.

of the stand-alone situation. In the parallel grid, the system cost approximately approaches the present cost of the A^2/O process. It can be found that bio-reactor dominates the system cost. Additionally, it is worth mentioning that the UASB reactor in our research can be easily scaled up with an extra economical investment to meet the expanded demand of the plant. This means that the cost of the reactor could be reduced while its size can be scaled for an increased wastewater capacity. The results reveal that a simulated improvement by using bio-hydrogen and a FC system is effective and feasible for the citric wastewater plant, even when compared to the current cost of the A^2/O process.

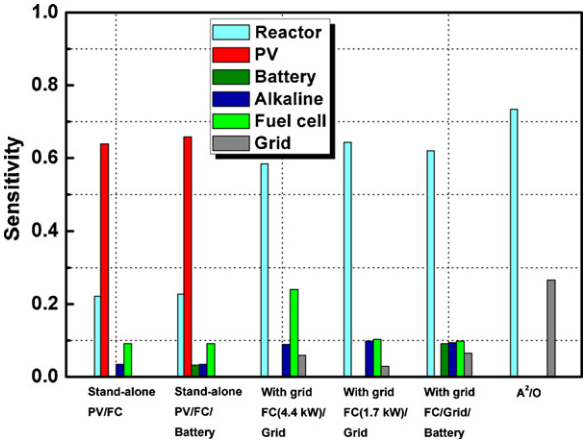

Fig. 12. Cost distribution of components in the system. The estimated cost is based on the vanadium battery.

4. Conclusions

Simulated improvements in a citric wastewater plant in meeting the dynamic load demand were developed. In this simulation, the hydrogen produced through the wastewater treatment process was utilized as the energy supply to a fuel cell. When considering the stand-alone situation, a PV array was employed because the fuel cell cannot meet the dynamic load demand individually. However, the system cost was much higher compared with the current A^2/O process because of the expense of the PV array. When comparing the PV-electrolyzer process and the PV-battery process, the hybrid configuration of FC and battery produced a higher overall system efficiency and lower system cost. Furthermore, a vanadium battery and lead acid battery were used to analyze the electricity storage. The vanadium battery demonstrated its superiority not only for cost but also the system efficiency in a long-running operation.

In the parallel grid, the system cost reached a comparable level when using the fuel cell as the energy supply. In particular, with a 1.7 kW rated fuel cell, the plant achieved a system cost of 0.238 US$ t^{-1}, which is lower than the cost of 0.257 US$ t^{-1} achieved by the A^2/O process. It is suggested that the utilization of hydrogen from wastewater treatment could be feasible, based on the economic analysis. When considering the cost distribution of components, the bio-reactor was found to be the major contribution to the total system cost. However the system cost could be further reduced, because the UASB reactor in our research can be easily scaled up when the capacity for wastewater is increased.

Acknowledgements

The authors would like to thank the Ministry of Science & Technology, China for financial support under the National Hi-Tech R&D Program (863 Program, Grant No. 2006AA05Z101) and Fraunhofer MAVO Adv. Energy Storage, Germany.

References

[1] E.M. Contreras, L. Giannuzzi, N.E. Zaritzky, Water Res. 34 (2000) 4455–4463.
[2] M.J. Rajczyk, Water Res. 27 (1993) 1257–1262.
[3] S.E. Oh, B.E. Logan, Water Res. 39 (2005) 4673–4682.
[4] S.W. Ginkel, S.E. Oh, B.E. Logan, Int. J. Hydrogen Energy 30 (2005) 1535–1542.
[5] P. Yang, R.H. Zhang, J.A. McGarvey, J.R. Benemann, Int. J. Hydrogen Energy 32 (2007) 4761–4771.
[6] H.J. Yang, P. Shao, T.M. Lu, J.Q. Shen, D.F. Wang, Z.N. Xu, X. Yuan, Int. J. Hydrogen Energy 31 (2006) 1306–1313.
[7] Fuel Cell Handbook, seventh edition, EG&G Technical Services, Inc., West Virginia, 2004.
[8] S.R. Vosen, J.O. Keller, Int. J. Hydrogen Energy 24 (1999) 1139–1156.
[9] C.H. Li, X.J. Zhu, G.X. Cao, S. Sui, M.R. Hu, Renew. Energy 34 (2009) 815–826.
[10] J.D. Maclay, J. Brouwer, G.S.T. Samuelsen, Int. J. Hydrogen Energy 31 (2006) 994–1009.
[11] J.D. Maclay, J. Brouwer, G. Scott Samuelsen, J. Power Sources 163 (2007) 916–925.
[12] E.M. Stewart, A.E. Lutz, S. Schoenung, et al., Int. J. Hydrogen Energy 34 (2009) 1638–1646.
[13] L. Hedstroem, C. Wallmark, P. Alvfors, M. Rissanen, B. Stridh, J. Ekman, J. Power Sources 131 (2004) 340–350.
[14] P. Hollmuller, J.M. Joubert, B. Lachal, K. Yvon, Int. J. Hydrogen Energy 25 (2000) 97–109.
[15] D. Shapiro, J. Duffy, M. Kimble, M. Pien, Solar Energy 79 (2005) 544–550.
[16] Rainer Lammertz Pure Gas Products, http://www.puregasproducts.com/hydrogenstorage50.htm (accessed December 2009).
[17] Ballard, http://www.ballard.com/ (accessed December 2009).

[18] W.J. Wang, PV Map of China, Institute of Electrical Engineering, Chinese Academy of Science, 2009 (accessed December 2009) http://www.martinot.info/Wang_WJ_GWREF2006.pdf.
[19] NAPS Power of Light, 2009 (accessed December 2009) http://www.napssystems.com/.
[20] Sandia, http://www.sandia.gov/ess/Publications/Conferences/2002/SCHOENING%20-%20ShortVsLongStorage.pdf (accessed December 2009).
[21] K.C. Divya, J. Ostergaard, Electr. Power Syst. Res. 79 (2009) 511–520.
[22] S.N. Hua, Q.S. Zhou, D.L. Kong, J.P. Ma, J. Power Sources 158 (2006) 1178–1185.
[23] C.G. Xie, S.X. Wang, L.H. Zhang, S.J. Hu, J. Power Sources 191 (2009) 433–441.
[24] Z.X. Liu, Z.M. Qiu, Y. Luo, Z.Q. Mao, C. Wang, Int. J. Hydrogen Energy 35 (2010) 2762–2766.